CONTROLLABILITY ANALYSIS AND STABILIZATION OF FLEXIBLE AIRCRAFTS

André Luís da Silva*, Takashi Yoneyama*, Pedro Paglione†

*ITA - Divisão de Engenharia Eletrônica
12.228-900, São José dos Campos, SP, Brasil

†ITA - Divisão de Engenharia Aeronáutica
12.228-900, São José dos Campos, SP, Brasil

Emails: andretaura@yahoo.com.br, takashi@ita.br, paglione@ita.br

Abstract— In this paper, we present a design methodology for a flight control system for a flexible aircraft. We investigate the controllability of flexible modes of the aircraft structure taking into account control constraints. Control channels are determined via examination of modal controllability and observability indices. A control law for the stabilization of unstable structural modes is designed via linear quadratic regulator, with feedback of selected outputs to respective control channels. All the design steps are performed assuming a linear aircraft model but the simulations are carried out using nonlinear model.

Keywords— Controllability Regions,Modal Controllability,Modal Observability,Flexible Aircraft Control

1 Introduction

Every aircraft is, in fact, a flexible body. However, an aircraft is commonly treated, in the flight mechanics and flight control, as a rigid body. More specifically, in the structural dynamics, the rigid body modes are commonly neglected. Such separation is acceptable when there are sufficient separation between rigid and flexible modes frequencies. However, trends in civil transport aircraft industry are leading to aircrafts with longer fuselages, larger aspect ratios, smaller thicknesses, composite material structures. Such configurations are more flexible than usual, so the flexible and rigid body modes frequencies tend to approximate, and integrated treatment for flight mechanics and structural dynamics should be considered.

In this paper, we present the design of a control system for the stabilization of flexible modes of a conceptual aircraft. This aircraft represents a medium size jet like EMBRAER 190/195 and Boeing 737-200/300 with augmented flexibility.

The aircraft possesses 8 aerodynamic control effectors. In order to verify if this arrangement is suitable to control the structural dynamics modes, controllability analyses are performed, via a formulation presented in (Goman and Demenkov, 2004), that takes into account the amplitude and rate constraints in the controls.

Elaboration of control channels is studied via modal controllability and observability indices, determined via a formulation presented in (Lindner et al., 1989).

The design of a control law, for a given choice of control channels, is performed via a simple LQR formulation, with static output feedback and gain matrix with predefined structure, presented in (Stevens and Lewis, 2003).

The controllability and observability analyses and the control design are performed with a linear approximation of the aircraft model. To verify the results, nonlinear simulations are performed.

2 Control Problem

2.1 Aircraft Model

The modeling of the flight mechanics of flexible aircraft have been discussed since the sixties, (Milne, 1964). Up to now, a variety of modeling approaches were elaborated, integrating different formulations for the aerodynamic, structural and inertial parts. A modeling approach that is interesting for flight control applications is presented in (Waszak and Schmidt, 1988). This approach is also considered in (Silvestre, 2007) and (Neto, 2008), taking into account, in each case, a more general aerodynamic formulation. The main hypothesis behind this approach is to assume small structural displacements, such that linear aerodynamics and structural dynamics can be considered. Also, the methodology is developed for aircrafts with traditional configurations, with aerodynamic forces and structural deformations more significant in the wing and empennages. In this approach, the structural dynamics that, in rigor, depends on time and space, depends only in time by taking a structural discretization via finite elements, with the choice of control points to evaluate the structural deformations. This discretization is followed by a modal decomposition that describes the displacements of these control points via the combination of vibration modes, (Bismarck-Nasr, 1999).

The model of the conceptual aircraft used in this work is presented in (da Silva et al., 2010), which is based in a technique presented in (Neto, 2008), which considers unsteady aerodynamics due to the structural vibration.

The general equations of motion are:

$$
\begin{aligned}
\dot{V} =& \frac{T}{m}\cos\alpha\cos\beta - \frac{D}{m} + g(\sin\phi\cos\theta\sin\beta + \\
& \cos\phi\cos\theta\sin\alpha\cos\beta - \cos\alpha\cos\beta\sin\theta) \qquad (1)
\end{aligned}
$$

$$
\begin{aligned}
\dot{\alpha} =& q - p\cos\alpha\tan\beta - r\sin\alpha\tan\beta - \frac{L}{mV\cos\beta} + \\
& \frac{g}{V\cos\beta}(\cos\phi\cos\theta\cos\alpha + \sin\alpha\sin\theta) \qquad (2)
\end{aligned}
$$

$$
\begin{aligned}
\dot{\beta} =& p\sin\alpha - r\cos\alpha + \frac{Y}{mV} - \frac{T}{mV}\sin\beta\cos\alpha + \\
& \frac{g}{V\cos\beta}(\sin\phi\cos\theta + \sin\theta\sin\beta\cos\beta\cos\alpha + \\
& -\sin\phi\cos\theta\sin^2\beta - \cos\phi\cos\theta\sin\alpha\sin\beta\cos\beta) \\
& \qquad (3)
\end{aligned}
$$

$$
\begin{aligned}
\dot{p} =& \frac{\left(I_{yy}I_{zz} - I_{zz}^2 - I_{xz}^2\right)qr + I_{xz}\left(I_{zz} - I_{yy} + I_{xx}\right)pq}{I_{xx}I_{zz} - I_{xz}^2} \\
& + \frac{I_{zz}\mathcal{L} + I_{xz}\mathcal{N}}{I_{xx}I_{zz} - I_{xz}^2} \qquad (4)
\end{aligned}
$$

$$
\dot{q} = \frac{I_{xz}r^2 + (I_{zz} - I_{xx})pr - I_{xz}p^2 + \mathcal{M} + \mathcal{M}_T}{I_{yy}} \qquad (5)
$$

$$
\begin{aligned}
\dot{r} =& \frac{I_{xz}\left(I_{yy} - I_{zz} - I_{xx}\right)qr + \left(I_{xz}^2 + I_{xx}^2 - I_{xx}I_{yy}\right)pq}{I_{xx}I_{zz} - I_{xz}^2} \\
& + \frac{I_{xz}\mathcal{L} + I_{xx}\mathcal{N}}{I_{xx}I_{zz} - I_{xz}^2} \qquad (6)
\end{aligned}
$$

$$
\ddot{\eta}_i + 2\zeta_i\omega_i\dot{\eta}_i + \omega_i^2\eta_i = \frac{Q_{\eta_i}}{\mu_i}, \quad i = 1, 2, \ldots n_m \qquad (7)
$$

Equations 1 to 6 are the rigid body equations of motion and Eq. 7 represents the structural dynamics. The six rigid body cinematic equations are not presented above, but are, of course, included in the model. V, α and β are the aircraft speed, angle of attack and sideslip angle, respectively. p, q and r are the roll, pitch and yaw rates, respectively. ϕ, θ and ψ are the bank, pitch and heading angles, respectively. η_i is the amplitude of the i^{th} vibration mode, in a set of n_m modes. L D and Y are the lift, drag and side aerodynamic forces, respectively. T is the thrust force. $\mathcal{L}$, $\mathcal{M}$ and $\mathcal{N}$ are the aerodynamic moments. $\mathcal{M}_T$ is the pitching moment due to thrust. m is the aircraft mass. Q_{η_i} is the generalized force in the i^{th} vibration mode. I_{xx}, I_{yy}, I_{zz} and I_{xz} are the aircraft inertias. g is acceleration due to gravity. ω_i is undamped natural frequency of the i^{th} vibration mode. μ_i and ζ_i are the generalized mass and generalized damping of the i^{th} vibration mode.

The scalar functions of time η_i are of abstract nature and dimensionless. These variables are defined such that the product $\eta_i\Sigma_i$ (where Σ_i is a constant vector called modal form of the i^{th} mode) gives the actual displacements of the control points in the structure due to the i^{th} vibration mode. The final structural deformation is given by the sum of $\eta_i\Sigma_i$ under all the modes considered. In figures 1 and 2, there are shown the modal forms of the 1^{st} and 2^{nd} vibration modes of the aircraft in question. For all the vibration modes considered in the model, the maximum element in the constant vector Σ_i is equal to 1 meter. So, $\eta_i = x$ means that the maximum structural deflection due to the i^{th} mode is equal to x meters.

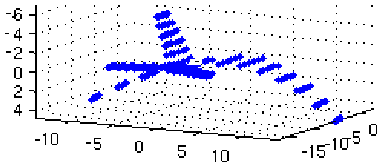

Figure 1: Modal form of the 1^{st} vibration mode.

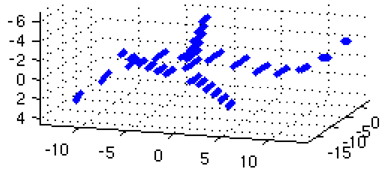

Figure 2: Modal form of the 2^{nd} vibration mode.

The forces L, D and Y, moments $\mathcal{L}$, $\mathcal{M}$ and $\mathcal{N}$ and generalized forces Q_{η_i} are functions linear on the control surfaces deflections and variables α, β, p, q, r, η_i, $\dot{\eta}_i$, $\ddot{\eta}_i$, $\eta_{lag,1_i}$ and $\eta_{lag,2_i}$. η_{lag,n_i} is called the n^{th} lag state with respect the i^{th} flexible mode. These states are inserted in the model to describe the unsteady aerodynamic effects, and the respective differential equations are in Eq. 8.

$$
\dot{\boldsymbol{\eta}}_{lag,n} = \dot{\boldsymbol{\eta}} - \frac{2V_e}{\bar{c}_w}\beta_n\boldsymbol{\eta}_{lag,n}, \quad n = 1, 2 \qquad (8)
$$

where $\boldsymbol{\eta}_{lag,n} = [\eta_{lag,n_1}\ \eta_{lag,n_2}\ \ldots\ \eta_{lag,n_{n_m}}]^T$, $\boldsymbol{\eta} = [\eta_1\ \eta_2\ \ldots\ \eta_{n_m}]^T$, V_e is the aircraft speed in some flight equilibrium condition, $\bar{c}_w$ is the aircraft mean aerodynamic chord, β_n is a parameter called lag term.

The aircraft possesses 8 aerodynamic controls plus the thrust control. This defines the control vector $\mathbf{u} = [\pi\ \delta_{ei}\ \delta_{eo}\ \delta_{asi}\ \delta_{aso}\ \delta_{aai}\ \delta_{aao}\ \delta_{rl}\ \delta_{ru}]^T$, where these controls, in the order of appearance: throttle setting, inboard elevator deflection, outboard elevator deflection, inboard aileron symmetric deflection, outboard aileron symmetric deflection, inboard aileron anti-symmetric deflection, outboard aileron anti-symmetric deflection, lower rudder deflection, upper rudder deflection.

2.2 *Control System Structure and Control Objectives*

The control objective is to stabilize the unstable flexible modes. For this purpose, first, it is necessary to verify if the flexible modes are controllable with limited deflections of the control surfaces. Controllability analyses are performed according an approach summarized in subsection 3.1.

In aircraft control, it is very difficult to perform state feedback. Also it is desired to feedback each output variable to predefined control channels.

Moreover, in aircraft control, it is important to design simple controllers. LQR formulation with static output feedback and control gain matrix with predefined structure is used in this work.

3 Theoretical Background

3.1 Controllability Regions

The controllability of linear systems is usually evaluated via the rank condition of a controllability matrix. This approach does not give an elucidative idea of degree of controllability. From the controllability definition, the rank condition only says if it exists or not a control such that, from any initial state, the origin can be reached in some time, given some tolerance in the rank computation or norm of the controllability gramian. In this case, there is no information about the practical feasibility of such control. As discussed in (Goman and Demenkov, 2004), if restrictions exists on the controls, limitations may exist in initial states from which the origin can be reached in some time.

In fact, in (Goman and Demenkov, 2004), for the following linear system:

$$\dot{\mathbf{x}}(t) = \mathbf{A}\mathbf{x}(t) + \mathbf{B}\mathbf{u}(t) \tag{9}$$

$$\left\{ \begin{array}{l} \mathbf{u}_{min} \le \mathbf{u}(t) \le \mathbf{u}_{max} \\ \dot{\mathbf{u}}_{min} \le \dot{\mathbf{u}}(t) \le \dot{\mathbf{u}}_{max} \end{array} \right. , \quad \forall t \ge 0 \tag{10}$$

with $\mathbf{x} \in \mathbb{R}^n$ and $\mathbf{u} \in \mathbb{R}^m$, it is considered the problem of find all the initial states such that:

$$\mathbf{x}(t) \to \mathbf{0}, \; \mathbf{u}(t) \to \mathbf{0}, \; \text{when } t \to \infty \tag{11}$$

As there exists constraints in the control rates, the controls are also states, so the problem is to find all the initial states in the augmented state space: $\mathbf{x}_a = (\mathbf{x}; \mathbf{u}) \in \mathbb{R}^{n+m}$. This set of initial states is named controllability region.

In (Goman and Demenkov, 2004), it is argued that the controllability region is strictly convex. Also, an optimization based approach is presented to find points in the boundary of this region. The approach consists in the maximization of the scalar function $\boldsymbol{\gamma}^T \mathbf{x}_{a_0}$, $\boldsymbol{\gamma}$ some constant vector, for $\mathbf{x}_{a_0}$ inside the controllability region. The result is one point contained in the boundary of the controllability region for each chosen direction $\boldsymbol{\gamma}$. To find these points in arbitrary directions may be not elucidative, so, it is considered the problem of find points for $\mathbf{x}_a$ constrained in some hyperplane defined by unit vectors $\mathbf{e}_i$ and $\mathbf{e}_j$ directed in the i^{th} and j^{th} axes of $\mathbb{R}^{n+m}$, respectively. This hyperplane is named "slice plane" and any respective point can be given as $(\mathbf{x}_0; \mathbf{u}_0) = \xi_1 \mathbf{e}_i + \xi_2 \mathbf{e}_j$. In this case, the problem is to maximize $\boldsymbol{\gamma}^T \boldsymbol{\xi}$, for $\boldsymbol{\gamma} \in \mathbb{R}^2$ and $\boldsymbol{\xi} = (\xi_1 \; \xi_2)^T$ keeping $(\mathbf{x}_0; \mathbf{u}_0)$ inside the intersection of the controllability region with the slice plane. The new maximization results, for each $\boldsymbol{\gamma}$, in a point in the boundary of this intersection.

In (Goman and Demenkov, 2004), it is shown that the optimization problem can be written as:

$$\max \boldsymbol{\gamma}^T \boldsymbol{\xi} \tag{12}$$

subject to:

$$(\mathbf{x}_0; \mathbf{u}_0) = \xi_1 \mathbf{e}_i + \xi_2 \mathbf{e}_j \tag{13}$$

$$\mathbf{x}_0 = -\int_0^T e^{-\mathbf{A}\tau} \mathbf{B}\mathbf{u}(\tau) d\tau \tag{14}$$

$$\mathbf{u}(\tau) = \mathbf{u}_0 + \int_0^\tau \dot{\mathbf{u}}(t) dt \tag{15}$$

$$\mathbf{u}_{min} \le \mathbf{u}(t) \le \mathbf{u}_{max} \tag{16}$$

$$\dot{\mathbf{u}}_{min} \le \dot{\mathbf{u}}(t) \le \dot{\mathbf{u}}_{max} \tag{17}$$

In Eq. 14, T is a finite final time. The original problem with infinite time is replaced for numerical feasibility of the optimization problem.

The optimization above is a mix of parametric and functional optimization, due to the necessity of find $\mathbf{u}(\cdot)$. In order to simplify this problem, in (Goman and Demenkov, 2004), a conservative approximation is made by considering the controls discretized via a first order holder. For this case, an algorithm can be implemented via linear programing, which also takes into account a Schur decomposition to divide the state space in stable and neutral and anti-stable portions, in order to eliminate numerical ill conditioning. Constraints in the state variables are also considered, in order to avoid unbounded controllability regions. An implementation of this algorithm was made in MATLAB, using the large scale function `linprog` of the MATLAB optimization toolbox.

3.2 Modal Controllability and Observability

In (Lindner et al., 1989), modal controllability and observability measures are presented. These measures are based on angles between the state space of a linear system and input and output spaces.

Consider the linear system in Eq. 9, with output given by $\mathbf{y} = \mathbf{C}\mathbf{x}$, $\mathbf{y} \in \mathbb{R}^l$. Let $\mathbf{p}_i$ and $\mathbf{q}_i$ be an right and left eigenvector, respectively, of matrix $\mathbf{A}$, with respect to its i^{th} eigenvalue. If all the eigenvalues are distinct, the following controllability and observability measures are defined.

$$\text{mc}_{ij} = \cos\Theta(\mathbf{q}_i, \mathbf{b}_j), \quad \text{mo}_{ij} = \quad \cos\Theta(\mathbf{p}_i, \mathbf{c}_j^T) \tag{18}$$

In Equation 18, mc_{ij} presents a modal controllability measure of the mode i with respect to the input j, mo_{ij} presents a modal observability measure of the mode i with respect to the output j. $\mathbf{b}_j$ is the j^{th} column of the matrix $\mathbf{B}$. $\mathbf{c}_j$ is the j^{th} row of the matrix $\mathbf{C}$. $\Theta(\mathbf{u}, \mathbf{v})$ denotes the angle between the vectors $\mathbf{u}$ and $\mathbf{v}$, in this case, a definition of the inner product shall be taken; we take the dot product, so that:

$$\mathrm{mc}_{ij} = \frac{\mathbf{q}_i^T \mathbf{b}_j}{||\mathbf{q}_i||\,||\mathbf{b}_j||},\ \mathrm{mo}_{ij} = \frac{\mathbf{c}_j \mathbf{p}_i}{||\mathbf{p}_i||\,||\mathbf{c}_j^T||} \tag{19}$$

where $||\cdot||$ denotes the Euclidean norm.

When one of these indices possess a value near 1, we expect strong controllability or observability. When they are near zero, we expect week controllability or observability.

It was also studied measures in (Tarokh, 1992). However, this approach determines indices that increase with the frequency of each mode. The frequency separation in the flexible aircraft is enough to give indices several orders of magnitude far from each other, that difficults the application.

3.3 LQR with Output Feedback

Consider the following control law via static output feedback, for the linear system of Eq. 9:

$$\mathbf{u} = -\mathbf{K}\mathbf{y},\ \mathbf{y} = \mathbf{C}\mathbf{x} \tag{20}$$

where $\mathbf{y} \in \mathbb{R}^l$ and $\mathbf{K}$ is a control gain matrix with predefined structure, so, with an arbitrary number of terms taken equal to zero.

The linear quadratic regulator approach can be used to determine the gains in matrix $\mathbf{K}$. Consider the following cost function to be minimized:

$$J = \int_0^\infty \mathbf{x}(t)^T \mathbf{Q}\mathbf{x}(t) + \mathbf{u}(t)^T \mathbf{R}\mathbf{u}(t)dt \tag{21}$$

$\mathbf{Q} \geq \mathbf{0}$, $\mathbf{R} > \mathbf{0}$.

In (Stevens and Lewis, 2003), it is shown that the solution of the optimization problem in question is given minimizing:

$$J' = \frac{1}{2}\mathrm{tr}(\mathbf{P}) \tag{22}$$

where:

$$\mathbf{A}_c^T\mathbf{P} + \mathbf{P}\mathbf{A}_c + \mathbf{C}^T\mathbf{K}^T\mathbf{R}\mathbf{K}\mathbf{C} + \mathbf{Q} = \mathbf{0} \tag{23}$$

$\mathbf{A}_c = \mathbf{A} - \mathbf{B}\mathbf{K}\mathbf{C}$ is the matrix "$\mathbf{A}$" in closed loop. Equation 23 is a Lyapunov equation, so that the matrix $\mathbf{A}_c$ shall be stable (all its eigenvalues shall have negative real parts). In this optimization, a stabilizing initial guess shall be provided and the minimization have to be conducted under the restriction that $\mathbf{A}_c$ remains stable.

An application in MATLAB was developed to implement the formulation in question, via the constrained minimization function `fmincon` of the optimization toolbox.

4 Application and Results

The aircraft presented in (da Silva et al., 2010) has 3 configurations of increasing flexibility. Here, we consider the second one that is conceived to possess more flexibility than most current aircrafts. Nine flexible modes are taken. The generalized dampings of the structure were adjusted to obtain unstable structural dynamics.

An equilibrium point for the nonlinear dynamics, around the flight condition altitude $H = 10000m$ and $V = 224.6m/s$, was determined. After, the linearization, via Taylor series truncation, around the equilibrium point was performed. The eigenvalues of the matrix $\mathbf{A}$ are presented in table 1. The eigenvalues related to the aerodynamic lag states are not shown. From table 1, the longitudinal dynamics (phugoid and short period) are stable. The lateral-directional dynamics has the spiral mode unstable. The first 5 flexible modes are unstable.

rigid body modes		flexible modes
$-0.767 \pm 2.281i$	short period	$0.8863 \pm 7.065i$
$-0.0017 \pm 0.0668i$	phugoid	$0.6139 \pm 12.32i$
-9.669×10^{-4}		$1.010 \pm 17.00i$
$-0.1542 \pm 1.369i$	dutch roll	$0.7025 \pm 17.01i$
-1.690	pure roll	$1.101 \pm 17.51i$
0.0038	spiral	$-0.040 \pm 19.26i$
		$-0.499 \pm 30.30i$
		$-0.365 \pm 33.36i$
		$-0.551 \pm 33.95i$

Table 1: Aircraft open loop poles.

To evaluate the controllability of this aircraft, described by this model, one can apply the controllability analysis approach of subsection 3.1, with the constraints in the controls presented in table 2. The computation of points in the boundary of the controllability region was carried out taking small final times T (between $4s$ and $6s$). They are small compared with the time constants of the phugoid mode. The discretization was performed with sampling rate near two times of the larger flexible mode undamped natural frequency. The restriction in T follows from computational issues. When this sampling rate is taken with a time T near the time constants of the phugoid mode, too many independent variables in the optimization (controls samples) result, so that `linprog` fails.

$0 \leq \pi \leq 1$	$\vert\dot{\pi}\vert \leq 5$	
$\vert\delta_{ei}\vert \leq 30^o$	$\dot{\delta}_{ei}$	$\leq 60^o/s$
$\vert\delta_{eo}\vert \leq 30^o$	$\dot{\delta}_{eo}$	$\leq 720^o/s$
$\vert\delta_{asi}\vert \leq 15^o$	$\dot{\delta}_{asi}$	$\leq 720^o/s$
$\vert\delta_{aso}\vert \leq 25^o$	$\dot{\delta}_{aso}$	$\leq 720^o/s$
$\vert\delta_{aai}\vert \leq 15^o$	$\dot{\delta}_{aai}$	$\leq 720^o/s$
$\vert\delta_{aao}\vert \leq 10^o$	$\dot{\delta}_{aao}$	$\leq 720^o/s$
$\vert\delta_{rl}\vert \leq 35^o$	$\dot{\delta}_{rl}$	$\leq 60^o/s$
$\vert\delta_{ru}\vert \leq 35^o$	$\dot{\delta}_{ru}$	$\leq 720^o/s$

Table 2: Control constraints

The considered slice planes are defined by the pairs: $\alpha-q$, $\beta-r$, $p-r$, $\phi-\beta$, $\eta_1-\dot{\eta}_1, \ldots\ \eta_9-\dot{\eta}_9$. In each case, the controllability boundaries are computed taking only 4 directions in the slice plane, all of them in one positive or negative direction of the respective axes. When different directions are taken, the optimization do not converge. In figure 3, we present the boundaries in the slice planes $\alpha - q$, $\beta - r$, $\eta_1 - \dot{\eta}_1$ and $\eta_2 - \dot{\eta}_2$. In this figure, Δ represents variation with respect to the equilibrium point. The plots show that initial conditions in $\Delta\alpha$ and β can extend up to 15^o, depending on combinations with q and r, respectively. Also, initial conditions in $\Delta\eta_1$ and η_2 can extend up to 3 (that correspond to $3m$). Due to space limitation, the boundaries in the remaining slice planes are not presented. However, these other boundaries also show good results. The evaluation confirms

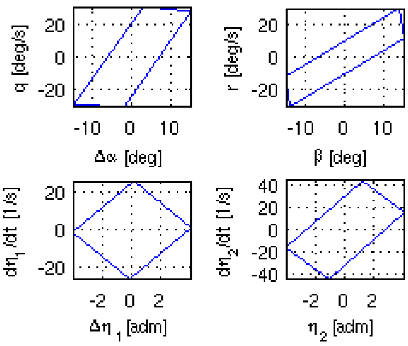

Figure 3: Controllability region boundaries.

the suitability of the current control arrangement to control rigid and flexible dynamics. However, prior control surfaces arrangements did not pass this test. In the development of the conceptual aircraft, first, were proposed ailerons with no symmetrical deflection. However, controllability analysis showed that this configuration was not suitable to control the first flexible mode. This problem was solved adopting symmetric deflections in the ailerons.

Applying the approach of modal controllability and observability presented in subsection 3.2, the modal controllability and observability indices were determined. Figure 4 presents controllability indices for all the modes less the aerodynamic lag modes, with respect all the controls less the throttle setting. The control related to each index is indicated. The modes are ordered as follows: 1-2 short period, 3-5 phugoid, 6-7 dutch roll, 8 pure roll, 9 spiral, 9+2i-10+2i i^{th} flexible mode. The numbers in the abscissa correspond to this enumeration of modes. Figure 5 presents observability indices for the same modes, grouped in the same way. Due to space restrictions, only the indices with respect to the outputs q, r, η_1 and $\dot{\eta}_1$ are presented. Although the model passed in the former controllability test, figure 4 shows that

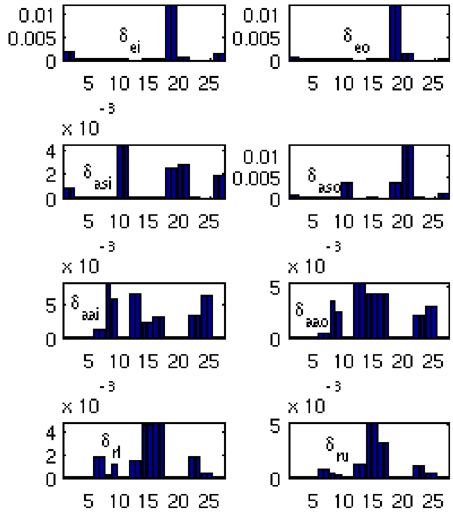

Figure 4: Controllability indices.

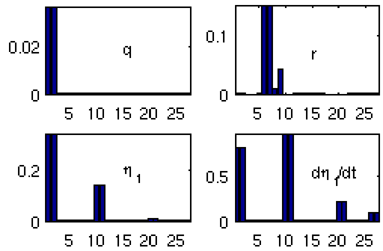

Figure 5: Observability indices.

all the controllability indices have apparent small values. Because of this, they are applied as relative measures to choose the control variables to control some mode. The results in the case of rigid body modes are consistent with the physical behavior in rigid body control, where "symmetric controls" (δ_{ei}, δ_{eo}, δ_{asi}, δ_{aso}) are more suitable for longitudinal modes and "anti-symmetric" controls (δ_{aai}, δ_{aao}, δ_{rl}, δ_{ru}) are more suitable for lateral-directional modes. In the flexible modes, symmetric controls are more suitable for the symmetric modes (vibration modes 1, 5, 6, 9) and anti-symmetric controls, more suitable for anti-symmetric modes (vibration modes 2, 3, 4, 7, 8).

Figure 5 shows well known properties of rigid body control, where the measurement of angular rate q is more suitable for short period control and of r is more suitable for lateral directional control. This figure also shows an important result for the flexible modes control, that is valid not only for the first vibration mode, but all the others: the best measurement to control the i^{th} vibration mode is the time rate of its modal amplitude.

As the first five vibration modes are unstable, one shall stabilize them. Also, one should stabilize the lateral-directional dynamics. Moreover, as usual in rigid body control, it was decided to augment the stability of the short period mode.

Bellow, are the chosen output variables and controls and the control channels, i.e., which output is sent to each control.

δ_{ei}	$\leftarrow$	q	δ_{aao}	$\leftarrow$	$\dot{\eta}_2$
δ_{eo}	$\leftarrow$	$\dot{\eta}_5$	δ_{rl}	$\leftarrow$	r
δ_{asi}	$\leftarrow$	$\dot{\eta}_1$	δ_{ru}	$\leftarrow$	$\dot{\eta}_3$, $\dot{\eta}_4$

Having defined the control channels, a structure was chosen for the control gain matrix and the formulation in subsection 3.3 was applied to compute the control gains. A diagonal matrix $\mathbf{Q}$ was taken with elements 2, 4, 6, 9, 10, 12, 14, 16 and 18 in the main diagonal equal to one and remaining equal to zero; and a diagonal matrix $\mathbf{R}$ with all the terms in the main diagonal equal to 10. As result, a stable closed loop system was obtained. In figure 6, the time responses of some rigid and flexible body variables are presented, computed with the nonlinear model, for a initial condition given by the sum of 5^o to the equilibrium values of α, β and ϕ. Although the control responses are not shown, they do not saturate.

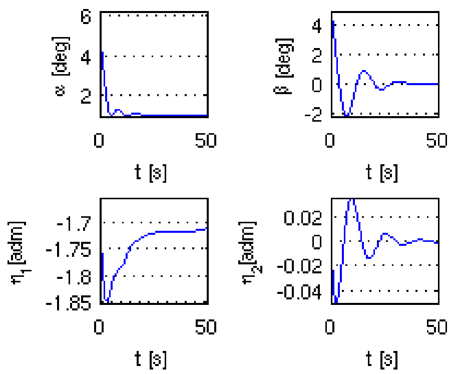

Figure 6: Closed loop response.

The nonlinear simulation proves the suitability of these linear techniques to this nonlinear case. However, the results are valid for sufficiently small regions around the design equilibrium point. In order to treat wider regions, gain scheduling may be applied, as commonly performed in the aircraft industry.

5 Conclusion

In this paper, we presented the development of a control system to stabilize a flexible aircraft with unstable structural dynamics.

A constrained controllability approach was applied to verify the control arrangement. The application resulted in changes on aircraft control configuration, what is very important in aircraft design.

Modal controllability and observability measures were applied to choose outputs, controls and define control channels. These choices are well understood in rigid body control. However, in flexible modes control, they may not be trivial and a straightforward approach is welcome instead of trial and error.

The design of a control law with static output feedback, via a LQR formulation, that implements the control channels, was presented. Nonlinear simulation shows the design effectiveness.

A nonlinear robust optimal control will be considered in future applications.

References

Bismarck-Nasr, M. N. (1999). *Structural Dynamics in Aeronautical Engineering*, American Institute of Aeronautics and Astronautics. ISBN 1563473232, 9781563473234.

da Silva, A. L., Paglione, P. and Yoneyama, T. (2010). Conceptual flexible aircraft model for modeling, analysis and control studies. Submitted for presentation in the 2010 AIAA Atmospheric Flight Mechanics Conference and Exhibit.

Goman, M. G. and Demenkov, M. N. (2004). Computation of controllability regions for unstable aircraft dynamics, *Journal of Guidance, Control, and Dynamics* **27**(4): 647–656.

Lindner, D. K., Babendreier, J. and Hamdan, A. M. A. (1989). Measures of controllability and observability and residues, *IEEE Transactions on Automatic Control* **34**(6): 648–650.

Milne, R. D. (1964). Dynamics of the deformable aeroplane, *Technical report*, London: Her Majesty's Stationery Office.

Neto, A. B. G. (2008). *Dinâmica e controle de aeronaves flexíveis com modelagem aerodinâmica pelo método doublet lattice*, Graduation final work, Technological Institute of Aeronautics (ITA), São José dos Campos, SP, Brazil. 176 p.

Silvestre, F. J. (2007). *Modelagem da mecânica de vôo de aeronaves flexíveis e aplicações de controle*, Master thesis, Technological Institute of Aeronautics (ITA), São José dos Campos, SP, Brazil. 115 p.

Stevens, B. L. and Lewis, F. L. (2003). *Aircraft Control and Simulation*, 2nd edn, John Wiley & Sons, Inc., chapter 5, pp. 403–419.

Tarokh, M. (1992). Measures for controllability, observability and fixed modes, *IEEE Transactions on Automatic Control* **37**(8): 1268–1273.

Waszak, M. R. and Schmidt, D. K. (1988). Flight dynamics of aeroelastic vehicles, *Journal of Aircraft* **25**(6): 563–571.